J Mater Sci (2015) 50:2700–2708
DOI 10.1007/s10853-015-8820-8

Bonding and high-temperature reliability of NiFeMo alloy/*n*-type PbTe joints for thermoelectric module applications

Haiyang Xia · Fivos Drymiotis · Cheng-Lung Chen · Aiping Wu · Yang-Yuan Chen · G. Jeffrey Snyder

Received: 21 August 2014 / Accepted: 3 January 2015 / Published online: 24 January 2015
© Springer Science+Business Media New York 2015

Abstract PbTe is an extremely important thermoelectric (TE) material, due to its high TE conversion efficiency. Consequently, our effort focuses on developing PbTe-based TE modules, which requires developing novel approaches for bonding metallic contacts to PbTe. In this study, Fe, Mo, and NiFeMo alloy foils were directly bonded to *n*-type PbTe using a rapid hot press at 600, 700, or 800 °C under a pressure of 40 MPa and for various holding times. We find that in the case of Fe and Mo, it is difficult to form a metallurgically bonded high strength joint with PbTe. However, we find that NiFeMo alloy does effectively bond to PbTe at 700 °C, but not at 600 °C. Significant liquid Pb, which might be due to the reaction of PbTe with Ni, is found that penetrates along the NiFeMo grain boundaries near NiFeMo/PbTe joints during bonding at 700 °C where the extent of liquid Pb penetration can be controlled with the time of bonding. Furthermore, the Seebeck coefficient of bulk PbTe with NiFeMo contacts is similar to that without NiFeMo contacts. Finally, the accelerated thermal aging of NiFeMo/PbTe elements at 600 °C for 240 h shows that the failure mechanism of NiFeMo/PbTe joints under operating conditions is the continued formation and penetration of eutectic liquid NiFeMo–PbTe and liquid Pb along the NiFeMo grain boundaries.

H. Xia (✉) · F. Drymiotis · C.-L. Chen · G. Jeffrey Snyder
Department of Materials Science, California Institute of Technology, 1200 E. California Blvd.,
Mail Code: 309-81, Pasadena, CA 91125, USA
e-mail: xhytsinghua@gmail.com; hyxia@caltech.edu

H. Xia · A. Wu
Department of Mechanical Engineering, Tsinghua University, Beijing 100084, China

H. Xia · A. Wu
Key Laboratory for Advanced Materials Processing Technology, Ministry of Education, Beijing, China

C.-L. Chen · Y.-Y. Chen
Institute of Physics, Academia Sinica, Taipei 11529, Taiwan

Introduction

PbTe-based thermoelectric (TE) materials are used to convert heat into electrical energy; mostly for space applications. The U.S. first used PbTe 2*n*/2*p*-based SNAP-3B radioisotope thermoelectric generators (RTGs) for Transit 4A and 4B in 1961. Then SNAP-9B RTGs based on PbTe 2*n*/2*p* were developed for Transit 5BN-1 and 5BN-2. From 1969 to 1972, NASA used SNAP-27 RTGs based on PbTe in Apollo 12 and 14–17 missions. Then improved SNAP-19 RTGs based on PbTe 2*n*/TAGS-85 were developed for Pioneer 10, 11, and Viking 1, 2. In 2011, NASA launched Mars Curiosity Rover which powered by MMRTG based on PbTe 2*n*/TAGS-85 [1, 2]. Although NASA has employed PbTe-based RTGs for several decades, there is not much detailed information about the electrical contacts to PbTe-based elements. According to some technical reports, NASA used Ni-plated Fe caps on the cold side and Fe cups on the hot side as the contacts to PbTe for SNAP-19 RTG and MMRTG. The direct mechanical connection method, spring and piston, was employed to connect the PbTe elements and the contacts [3, 4]. However, this method is complicated and leads to low efficiency of the TE device. Furthermore, PbTe-based TE devices can be employed for terrestrial applications, such as automotive and industry waste heat recovery. The direct mechanical connection method has no advantage for mass production. Some researchers from Japan bonded

PbTe to Ni contacts by plasma activated sintering, but there was no detailed analysis of the interfacial microstructure of the PbTe contacts [5].

For a good PbTe-based TE contacts, several requirements must be met, which have been discussed in our previous paper [6]. Our previous research on Ni/PbTe joints showed that Ni bonds well to PbTe but reacts quickly with PbTe [6] and therefore we are exploring alternative materials. We decided to investigate the bonding properties of Fe/PbTe and Mo/PbTe and subsequently those of a NiFeMo alloy. The NiFeMo alloy may work as a good interlayer since contains the reactive Ni but also the non-reactive (according to the literature [7]) Fe and Mo. The Fe and Mo in NiFeMo alloy might inhibit the reaction of Ni with PbTe, which might increase the operating temperature and prolong the lifetime of the joints.

In this study, NiFeMo alloy foil was directly bonded to *n*-type PbTe by one-step hot-press sintering. The resulting interfacial microstructures of the NiFeMo/PbTe joints are investigated and the phases and the distribution of elements at the NiFeMo/PbTe interface are analyzed. The obtained data are used to get the optimal bonding parameters and estimate the quality of the NiFeMo/PbTe joints. The Seebeck coefficients of bulk PbTe with and without NiFeMo contacts are measured to study the effect of the bonding process on the TE properties of PbTe. Additionally, an accelerated thermal aging experiment of NiFeMo/PbTe TE elements is conducted in order to determine the failure mechanism and estimate the lifetime of the NiFeMo/PbTe joints.

Experimental procedure

Polycrystalline $PbTe_{0.9988}I_{0.0012}$ samples were prepared by melting and annealing. Stoichiometric mixtures of high-purity Pb, Te, and PbI_2 were sealed in graphite-coated quartz ampoules under vacuum and heated to 1000 °C. After holding at 1000 °C for 6 h, the ampoules were cold-water quenched and annealed at 700 °C for 48 h. The resulting *n*-type PbTe ingots were then ground into powders by ball milling in an inert atmosphere. The Fe foil, Mo foil with a thickness of 100 μm and the NiFeMo alloy (82 Ni wt%, 15 Fe wt% and 3 Mo wt%) foil with a thickness of 150 μm were first polished by SiC sandpaper with 240, 400, 600, and finally 800 grits, and then cleaned with acetone and then isopropanol in an ultrasonic bath. Subsequently, the foils and *n*-type PbTe powders were placed into a graphite die and were assembled into the layered structure Fe/PbTe/Fe, Mo/PbTe/Mo, and NiFeMo/PbTe/NiFeMo, respectively. The TE elements were sintered by a rapid hot press with argon flow and under a pressure of 40 MPa at 600, 700, or 800 °C for 60, 150, or 300 min. The specimens were cooled in the chamber by flowing inert gas. The samples were cooled below 400 °C for several minutes and to room temperature for around 1 h. After bonding, a part of the NiFeMo/PbTe/NiFeMo TE elements bonded at 700 °C for 60 min was encapsulated in an evacuated silica tube and was aged at 600 °C for 240 h. Both as-bonded and post-aged samples were cut into cross sections and polished in order to investigate the microstructures of the joints by scanning electron microscope (SEM, ZEISS 1550VP) at Caltech. The distributions of elements were determined by X-ray energy dispersive spectrometer (EDS, Oxford X-Max), and the EDS software AztecEnergy (Oxford Instrument) with the library standards provided by the EDS software vendor was used to transform the EDS line scanning intensity data to composition data. The precise composition of the phases at the interface was detected by an electron-probe micro analyzer (EPMA, JEOL JXA-8200) with independent compositional standards at Caltech. The Seebeck coefficients of bulk PbTe with and without NiFeMo contacts were tested by the high-temperature Seebeck coefficient measurement system at Caltech [8].

Results and discussion

Bonding of pure Fe and Mo foils to *n*-type PbTe

We attempted to bond pure Fe and Mo foils to *n*-type PbTe by a rapid hot press at 600, 700, and 800 °C. Pure Mo foil failed to bond and no reaction product was detected at the Mo/PbTe surface. A joint with very poor strength formed at 800 °C at the Fe/PbTe interface. Figure 1a shows the back-scattered electron (BSE) micrograph at the interface of Fe/PbTe joints which were bonded at 800 °C for 60 min. It can be observed that no reaction product formed at the interface. Figure 1b corresponds to the EPMA result at the interface of Fe/PbTe joints that is shown in Fig. 1a. It shows that during the joint bonding process, Fe atoms diffused a distance of approximately 20 μm into the PbTe.

Although tellurides of Fe and Mo exist, no reaction is expected with PbTe as we observed. Based on the Fe–Te [9] and Mo–Te [10] binary phase diagrams, several binary phases are found to be stable within these systems, including $Fe_{1.12}Te$ (β), $Fe_{0.67}Te$ (δ), $FeTe_2$ (ε), Mo_3Te_4, and $MoTe_2$ (α). Table 1 lists the formation Gibbs free energy ($\Delta_f G_T$) of $Fe_{1.12}Te$ (β), $Fe_{0.67}Te$ (δ), $FeTe_2$ (ε), Mo_3Te_4, $MoTe_2$ (α), and PbTe based on the literatures [11–13]. Table 2 contains the calculated results of the reaction Gibbs free energy ($\Delta_r G_T$) of the reaction of Fe with PbTe and the reaction of Mo with PbTe. The calculations show that no binary phase can form during the reaction of either Fe or Mo with PbTe due to the positive reaction Gibbs free

energy. This is in agreement with our experimental observation. Even though Fe and Mo do not form a metallurgically bonded high strength joint with PbTe, it may be possible that they can be used to reduce the reaction rate of some metals with PbTe; for example Ni/PbTe.

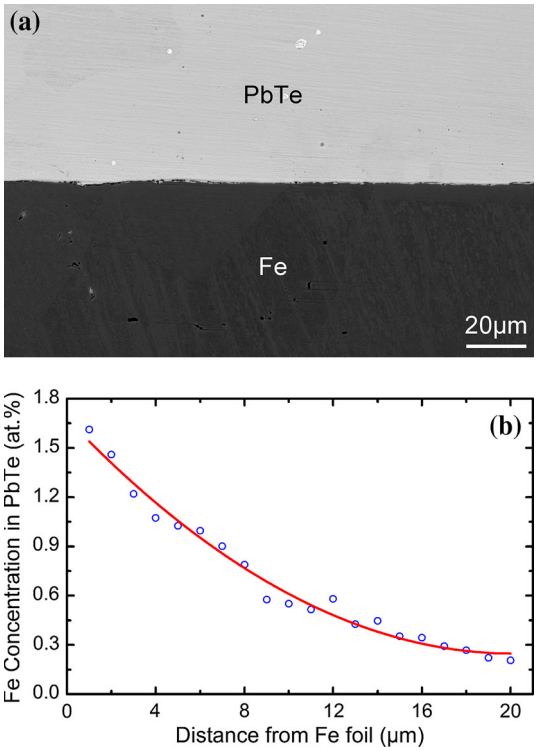

Fig. 1 **a** SEM micrograph of the interface of Fe/PbTe joints bonded at 800 °C for 60 min; **b** EPMA result of Fe concentration in PbTe from the interface between Fe foil and PbTe

Bonding of NiFeMo alloy foil to *n*-type PbTe

Figure 2a, b shows the BSE micrographs at the interface of the NiFeMo/PbTe joints that were bonded at 600 °C for 300 min. The micrographs reveal the presence of a porous layer with cracks between the NiFeMo foil and PbTe,

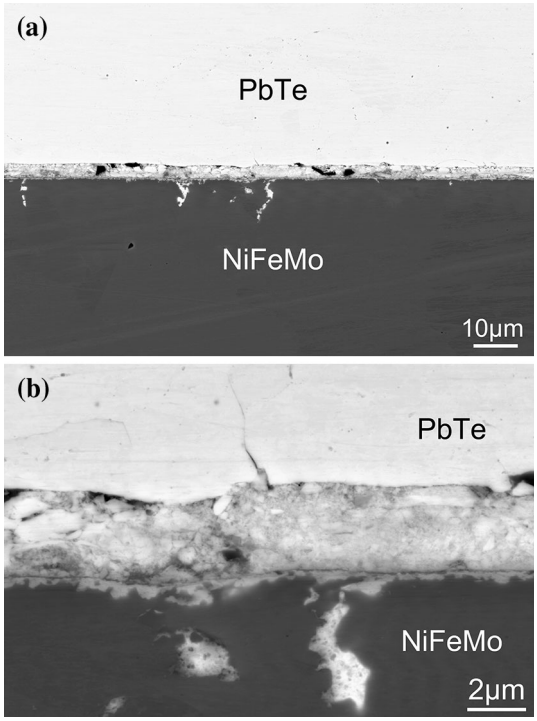

Fig. 2 SEM micrographs of the interface of NiFeMo/PbTe joints bonded at 600 °C for 300 min

Table 1 Thermodynamic data of $Fe_{1.12}Te$, $Fe_{0.67}Te$, $FeTe_2$, Mo_3Te_4, $MoTe_2$, and PbTe

Phase label	Formula in reference	Formula used here	Temperature (K)	$\Delta_f G_T$ (kJ/mol)	Reference
$Fe_{1.12}Te$-β	$FeTe_{0.9}$	$Fe_{1.12}Te$	1100	−23.458	[11]
$Fe_{0.67}Te$-δ	$Fe_{0.67}Te$	$Fe_{0.67}Te$	1000	−21.610	[12]
$FeTe_2$-ε	$FeTe_2$	$Fe_{0.5}Te$	900	−18.527	[11]
Mo_3Te_4	Mo_3Te_4	$Mo_{0.75}Te$	1100	−38.057	[13]
$MoTe_2$-α	$MoTe_2$	$Mo_{0.5}Te$	1100	−32.942	[13]
PbTe	PbTe	PbTe	900	−56.067	[11]
			1000	−51.630	[11]
			1100	−47.107	[11]

Table 2 Calculated thermodynamic data of the reaction of Fe with PbTe and the reaction of Mo with PbTe

Chemical reaction equation	Temperature (K)	$\Delta_r G_T$ (kJ/mol)
1.12 Fe + PbTe → $Fe_{1.12}Te$ + Pb	1100	17.649
0.67 Fe + PbTe → $Fe_{0.67}Te$ + Pb	1000	30.020
0.5 Fe + PbTe → $Fe_{0.5}Te$ + Pb	900	37.540
0.75 Mo + PbTe → $Mo_{0.75}Te$ + Pb	1100	9.050
0.5 Mo + PbTe → $Mo_{0.5}Te$ + Pb	1100	14.165

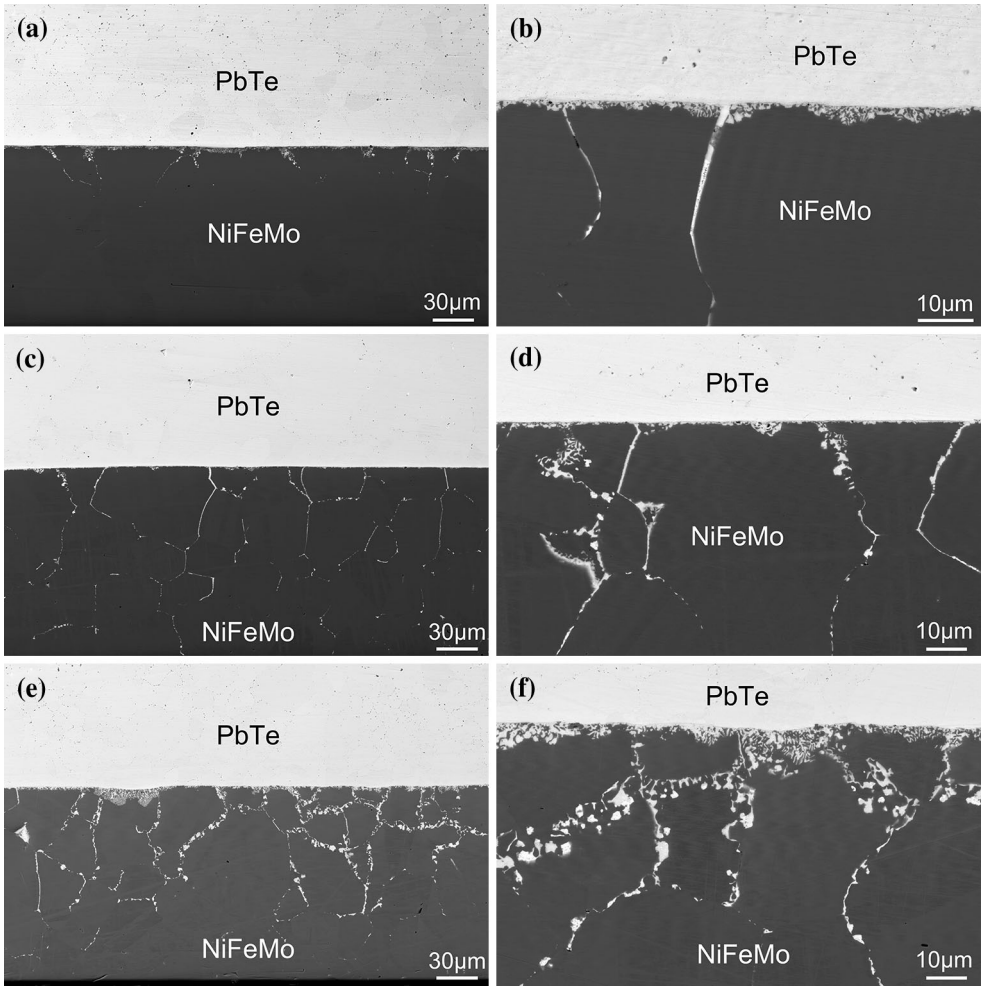

Fig. 3 SEM micrographs of the interface of NiFeMo/PbTe joints bonded at 700 °C for **a**, **b** 60 min; **c**, **d** 150 min; and **e**, **f** 300 min

which indicates that at 600 °C the NiFeMo alloy foil does not make a good bond with PbTe. Figure 3a, b shows the BSE micrographs at the interface of the NiFeMo/PbTe joints that were bonded at 700 °C for 60 min. Under these conditions, the NiFeMo alloy foil bonds well to *n*-type PbTe. No porous layer can be found between the NiFeMo alloy foil and PbTe. However, some material, which presumably consists mostly of PbTe, slightly diffuses into the NiFeMo grain interiors and the NiFeMo grain boundaries. Figure 3c, d shows the BSE micrographs at the interface of the NiFeMo/PbTe joints bonded at 700 °C for 150 min. With increasing bonding time, the aforementioned material diffuses nearly throughout the NiFeMo alloy foil, along its grain boundaries. The BSE micrographs at the interface of the NiFeMo/PbTe joints bonded at 700 °C for 300 min are shown in Fig. 3e, f. The micrographs show that the width of the material along the NiFeMo grain boundaries becomes larger, which will eventually lead to the separation of the NiFeMo grains and the subsequent failure of the joint.

Figures 4 and 5 show the EDS mapping and line scanning results of the interface of NiFeMo/PbTe joints that were bonded at 700 °C for 300 min. The microstructure presented in Fig. 4a suggests that a eutectic liquid phase between NiFeMo foil and PbTe might form during the bonding process. The melting point of PbTe is 924 °C, and based on the literature, the eutectic temperature of Fe–PbTe (16 at.% Fe) is 857 °C [14] while the eutectic temperature of Ni–PbTe (8 at.% Ni) is 624 °C [15]. According to our bonding experiment of Fe/PbTe joints, the eutectic temperature of PbTe–Fe should be above 800 °C, which is consistent with the aforementioned literature value. Additionally, in our previous study of Ni/PbTe joints [6], a liquid phase formed at the Ni/PbTe interface at 650 °C, which subsequently led to the formation of a ternary phase. Further investigation of the Ni/PbTe interface revealed that the liquid phase forms rapidly at interface, and at 700 °C the Ni foil dissolves into the liquid at a high rate. Consequently, the Ni foil will disappear because the liquid phase will be extruded out under the bonding pressure. Based on

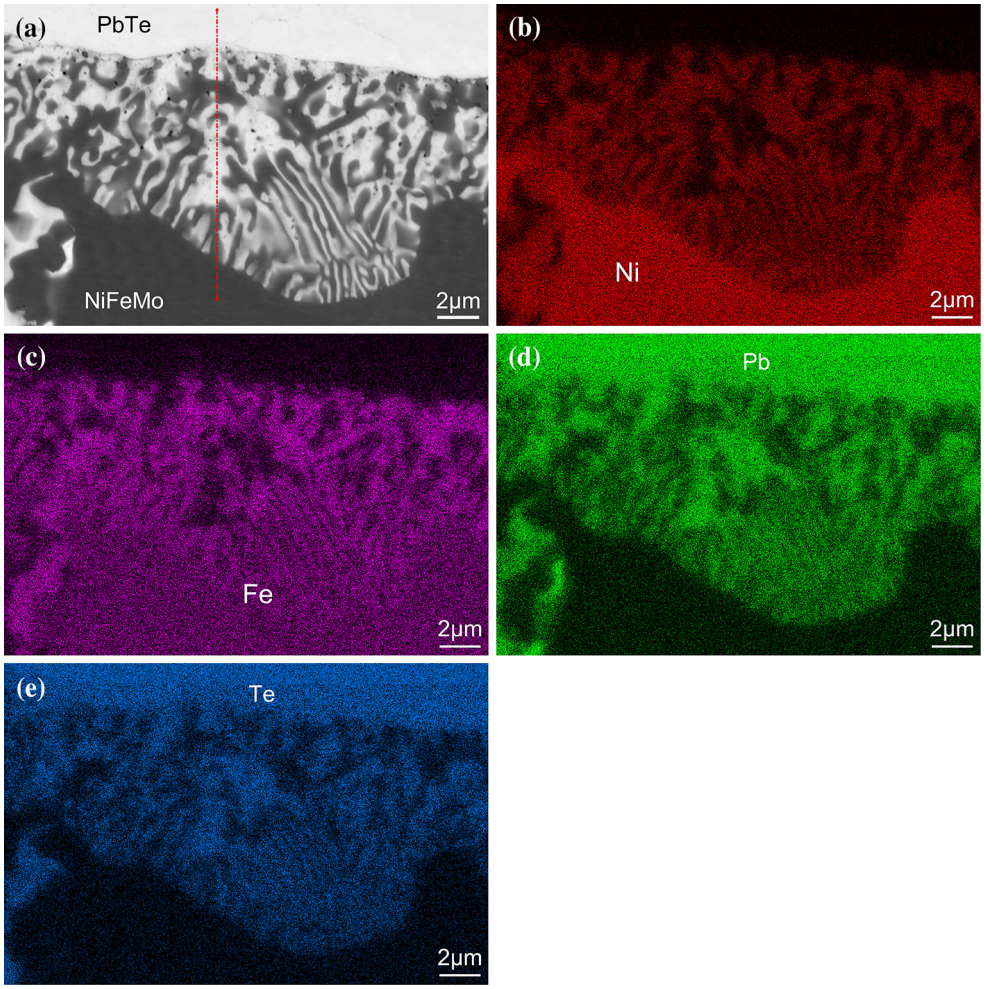

Fig. 4 SEM micrograph and EDS mapping images of the interface of NiFeMo/PbTe joints bonded at 700 °C for 300 min: **a** SEM micrograph, **b** Ni element mapping, **c** Fe element mapping, **d** Pb element mapping, and **e** Te element mapping

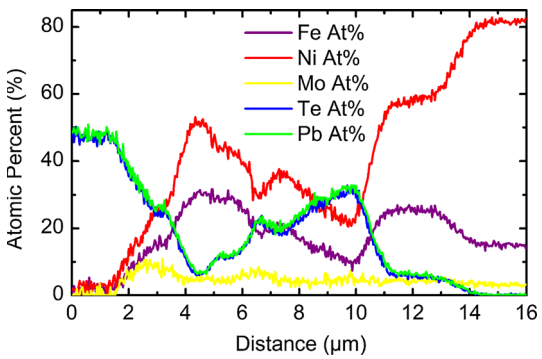

Fig. 5 EDS line scanning result of the interface of NiFeMo/PbTe joints bonded at 700 °C for 300 min shown in Fig. 4a

this information, we conclude that the eutectic temperature of Ni–PbTe should be below 700 °C, which is in agreement with the literature value. Hence, due to the similarity of Ni and NiFeMo, we anticipate that a eutectic liquid phase will also form between the NiFeMo alloy and PbTe, but at a higher temperature. The higher eutectic temperature, due to the presence of Fe and Mo, suggests that the NiFeMo/PbTe joints should have a higher operation temperature compared to Ni/PbTe joints.

Figures 6 and 7 show the EDS mapping and line scanning results of the NiFeMo grain boundary region of NiFeMo/PbTe joints bonded at 700 °C for 300 min. Both PbTe and Pb are observed in this region. The formation of liquid Pb is presumably caused by the reaction of PbTe with NiFeMo and/or the decomposition of PbTe. Although no apparent reaction products, like nickel telluride, are observed at the NiFeMo/PbTe joints, it can not be concluded that there is no reaction between PbTe and NiFeMo; the reaction products might be too small to be detected. What is observed though is that a lot of liquid Pb forms and penetrates along the NiFeMo grain boundaries at the NiFeMo/PbTe joints. This is similar to the microstructure developed at the Ni/PbTe joints [6].

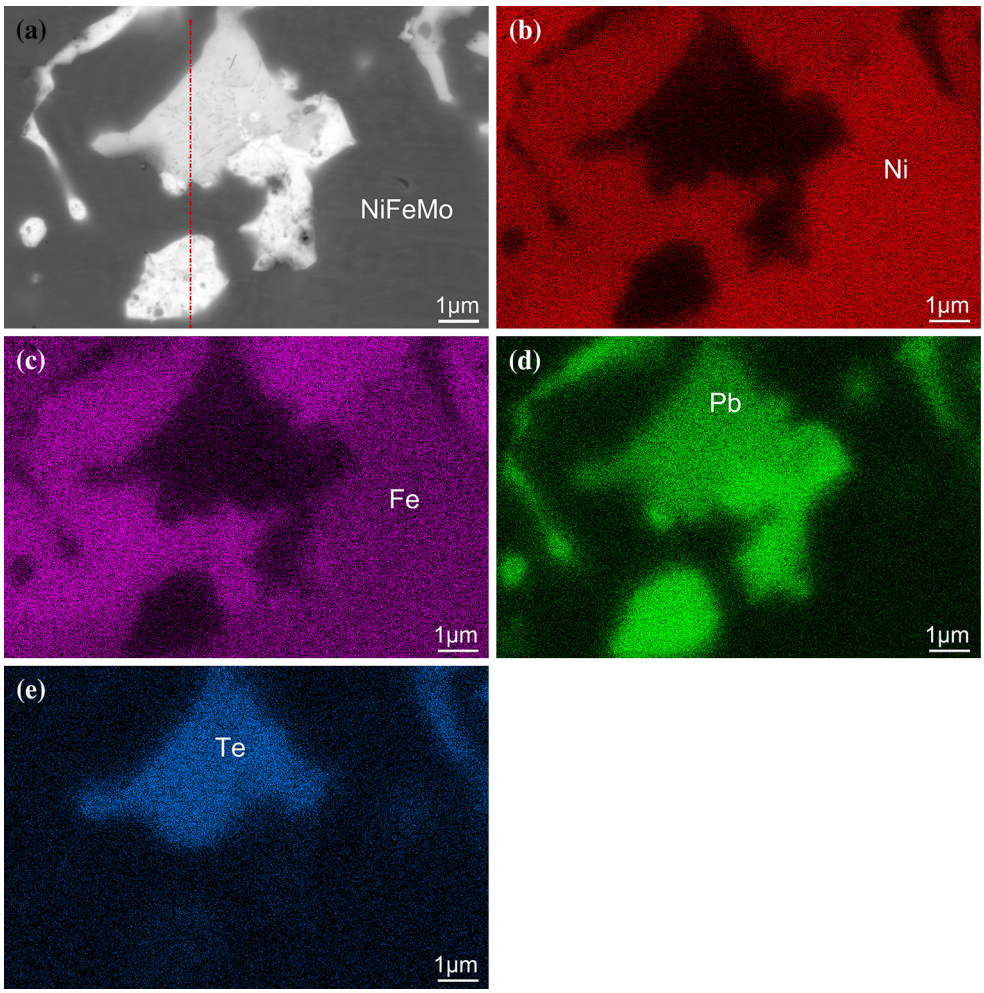

Fig. 6 SEM micrograph and EDS mapping images of the NiFeMo grain boundaries at the NiFeMo/PbTe joints bonded at 700 °C for 300 min: **a** SEM micrograph, **b** Ni element mapping, **c** Fe element mapping, **d** Pb element mapping, and **e** Te element mapping

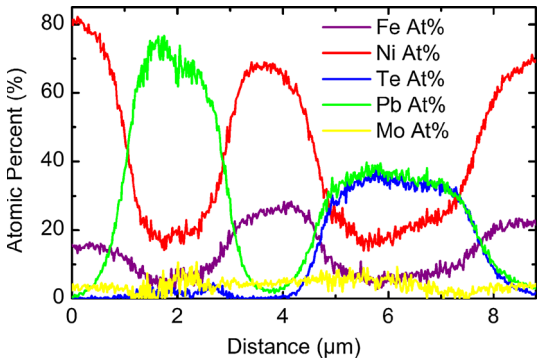

Fig. 7 EDS line scanning result of the NiFeMo grain boundaries at the NiFeMo/PbTe joints bonded at 700 °C for 300 min shown in Fig. 6a

The formation of the microstructures of NiFeMo/PbTe joints bonded at 700 °C might be caused by two reasons. The main reason might be the eutectic liquid phase formed at the NiFeMo/PbTe interface and along the NiFeMo grain boundaries and the formed liquid phase NiFeMo–PbTe infiltrated into the NiFeMo grain boundaries under the high pressure (40 MPa) during the bonding process. That is why PbTe distributed along the NiFeMo grain boundaries. The secondary reason might be the liquid Pb caused by the reaction of PbTe with NiFeMo and/or the decomposition of PbTe penetrated along the NiFeMo grain boundaries and accelerated the NiFeMo–PbTe melt infiltration. According to the theory of liquid metal penetration (LMP), also named as liquid metal embrittlement (LME) or grain boundary penetration (GBP), the liquid material will penetrate along the grain boundaries of solid material when $2\gamma_{SL} < \gamma_{GB}$, where γ_{SL} is the interfacial energy between solid material and liquid material and γ_{GB} is the grain boundary energy of the solid material. However, the mechanism of LMP is still under study and is likely related to the types of the materials [16]. The penetration process depends on many factors, such as the solubility of the solid element in the liquid

Table 3 Solubility of Ni, Fe and Mo in liquid Pb

Solid metal	Temperature (°C)	Experimental solubility		Reference	Calculated solubility		Reference
		wt%	at.%		wt%	at.%	
Ni	600	0.52	1.81	[18]	0.59	2.06	[19]
	700	0.76	2.63	[18]	0.87	3.00	[19]
Fe	600	2.44×10^{-4}	9.05×10^{-4}	[18]	1.34×10^{-4}	4.98×10^{-4}	[19]
	700	6.23×10^{-4}	23.1×10^{-4}	[18]	5.53×10^{-4}	20.5×10^{-4}	[19]
Mo	600	$<10^{-6}$	–	[18]	–	–	–
	700	$<10^{-6}$	–	[18]	–	–	–

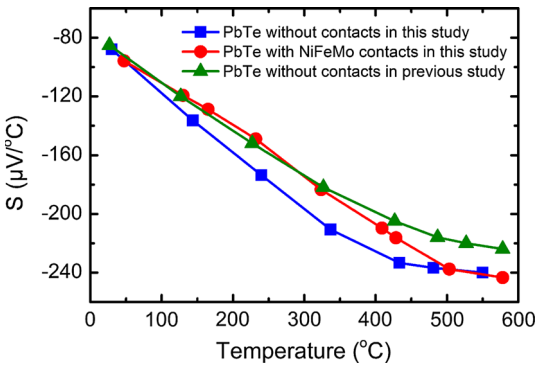

Fig. 8 Seebeck coefficients of bulk PbTe with NiFeMo contacts bonded at 700 °C for 120 min, bulk PbTe without NiFeMo contacts sintered at 600 °C for 30 min in this study and bulk PbTe without NiFeMo contacts sintered at 550 °C for 60 min in previous study

material C_{SL}, the diffusivity of the solid element in the liquid material D_{SL}, the solid–liquid interfacial energy γ_{SL}, the grain boundary energy of solid material γ_{GB}, the solid grain boundary self-diffusion coefficient D_{GB}, temperature T and time t [17]. Table 3 lists the solubility of Ni, Fe, and Mo in liquid Pb, which shows that the solubility of Ni in liquid Pb is about 1000 times than that of Fe in liquid Pb, and is about 10^6 times than that of Mo in liquid Pb. Hence, liquid Pb would easily penetrate into the grain boundaries of Ni, while liquid Pb is difficult to penetrate into the grain boundary of Mo. Fe has an intermediate resistance to the penetration of liquid Pb [20, 21]. Additionally, the pressure plays a crucial role in the penetration rate. Within a certain scope, a high pressure can accelerate the penetration rate.

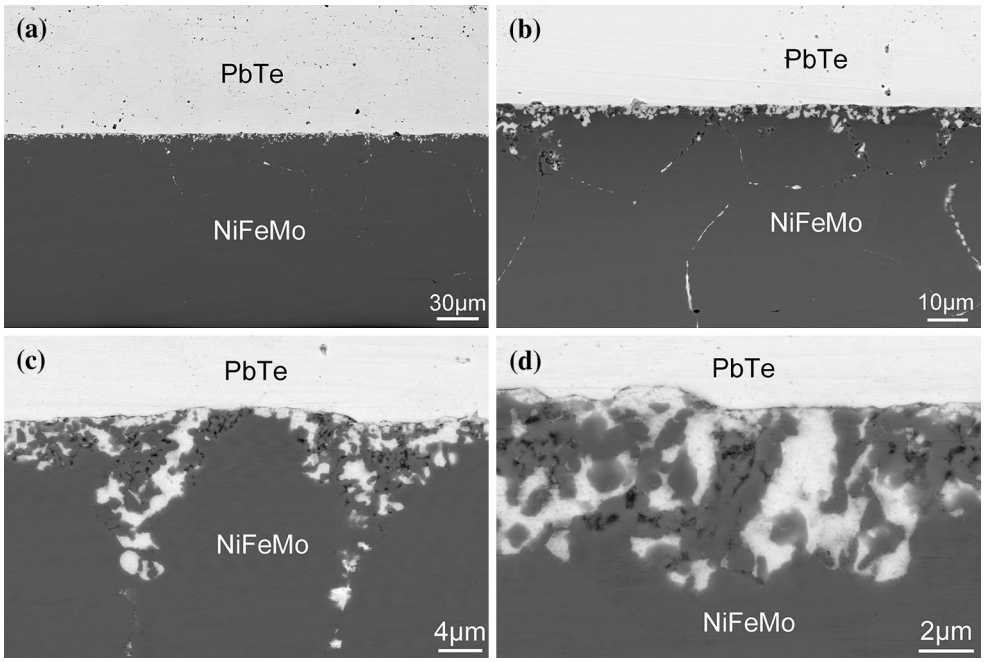

Fig. 9 SEM micrographs of the interface of NiFeMo/PbTe joints bonded at 700 °C for 60 min after accelerated aging at 600 °C for 240 h

Effect of bonding process on the Seebeck coefficient of bulk PbTe TE materials

Compared to the sintering temperature used for the fabrication of bulk PbTe samples without contacts, commonly about 500–600 °C, the bonding temperature 700 °C used in this study is higher and might affect the Seebeck coefficient. In addition, the interdiffusion and interface between NiFeMo foil and PbTe might also have an effect on the Seebeck coefficient of bulk PbTe. Thus, in order to investigate the effect of the bonding process, the Seebeck coefficients of bulk *n*-type PbTe without NiFeMo contacts sintered at 600 °C for 30 min and bulk NiFeMo/*n*-type PbTe/NiFeMo TE element bonded at 700 °C for 150 min were measured, from room temperature to 600 °C. The measured results are shown in Fig. 8. The Seebeck coefficient of bulk PbTe without contacts sintered at 550 °C for 60 min in our previous study [22] is also shown in Fig. 8 for comparison. There is no significant difference between the Seebeck coefficients of these samples, which suggests that the bonding parameters used in this study are appropriate for bonding NiFeMo foil onto *n*-type PbTe.

Accelerated thermal aging of NiFeMo/PbTe TE element

The hot side of the PbTe-based TE element commonly operates at 500–550 °C for several months to decades. For example, the hot side operation temperature of PbTe-based TE modules used in MMRTG is about 538 °C. Above 500 °C, the sublimation, oxidation (if in air), and decomposition of PbTe will become severe and lead to the degradation of the TE properties of PbTe. The sublimation rate constant of PbTe at 500 °C is about 9.4×10^{-2} g/cm^2 h [23]. In order to investigate the high-temperature reliability of NiFeMo/PbTe joints, an accelerated thermal aging test at 600 °C was conducted in vacuum. Figure 9 shows the BSE micrographs of the interface of NiFeMo/PbTe joints, which were bonded at 700 °C for 60 min and then aged at 600 °C for 240 h. The microstructure is similar with the as-bonded joints. However, the formation and penetration rate of eutectic liquid NiFeMo–PbTe and liquid Pb at 600 °C without pressure is very slower than that at 700 °C under 40 MPa pressure. That is because the pressure can accelerate the melt infiltration during the bonding process. According to our observations, the failure mechanism of NiFeMo/PbTe joints under operation temperature is the continued formation and penetration of eutectic liquid NiFeMo–PbTe and liquid Pb along the NiFeMo grain boundaries, which will lead in the separation of NiFeMo and subsequent contact degradation. If a long lifetime is required for NiFeMo/PbTe joints, the hot side operation temperature should not be above 500 °C.

Conclusions

Fe and Mo foils are difficult to form a metallurgical bonded high strength joint with PbTe. The thermodynamic calculations show that no binary phase can form during the reaction of Fe or Mo with PbTe. NiFeMo alloy does not effectively bond to PbTe at 600 °C, but it does bond at 700 °C. Significant liquid Pb forms and penetrates along the NiFeMo grain boundaries at NiFeMo/PbTe joints at 700 °C. The Seebeck coefficient of bulk PbTe with NiFeMo contacts is similar with that without NiFeMo contacts, indicating the bond does not adversely affect the TE properties. The accelerated thermal aging of NiFeMo/PbTe elements at 600 °C for 240 h shows that the failure mechanism of NiFeMo/PbTe joints under operation temperature is the continued formation and penetration of eutectic liquid NiFeMo–PbTe and liquid Pb along the NiFeMo grain boundaries.

Acknowledgements Haiyang Xia thanks for the support of Tsinghua Visiting Doctoral Students Foundation and the Opening Project of State Key Laboratory of Advanced Brazing Filler Metals & Technology (Zhengzhou Research Institute of Mechanical Engineering). This work was supported under the DOW bridge program at Caltech.

References

1. Abelson RD (2006) Space missions and applications. In: Rowe DM (ed) Thermoelectric handbook: macro to nano. CRC Press, Boca Raton, pp 56–57
2. LaLonde AD, Pei YZ, Wang H, Snyder GJ (2011) Lead telluride alloy thermoelectrics. Mater Today 14:526–532
3. Isotopes nuclear system division (1969) TAGS-85/2N RTG power for Viking lander capsule. Teledyne Company, Baltimore
4. Caillat T (2005) Advanced thermoelectric power generation technology development at JPL. In: 3rd European conference on thermoelectrics, September 2005, Nancy, France
5. Orihashi M, Noda Y, Chen LD, Kang YS, Moro A, Hirai T (1998) Ni/*n*-PbTe and Ni/p-$Pb_{0.5}Sn_{0.5}Te$ joining by plasma activated sintering. In: Proceedings of 17th international conference on thermoelectrics, Nagoya, Japan, p 543
6. Xia HY, Drymiotis F, Chen CL et al (2014) Bonding and interfacial reaction between Ni foil and *n*-type PbTe thermoelectric materials for thermoelectric module applications. J Mater Sci 49:1716–1723. doi:10.1007/s10853-013-7857-9
7. Eiss AL (1966) Thermoelectric bonding study. NASA, Washington, DC
8. Iwanaga S, Toberer ES, LaLonde A, Snyder GJ (2011) A high temperature apparatus for measurement of the Seebeck coefficient. Rev Sci Instrum 82:063905
9. Okamoto H, Tanner LE (1990) Fe–Te (iron–tellurium). In: Massalski TB (ed) Binary alloy phase diagrams. ASM International, Materials Park, pp 1781–1783
10. Brewer L, Lamoreaux RH (1990) Mo–Te (molybdenum–tellurium). In: Massalski TB (ed) Binary alloy phase diagrams. ASM International, Materials Park, pp 2675–2676
11. Barin I (1995) Thermochemical data of pure substances, 3rd edn. VCH, Weinheim

12. Ball RGJ, Dickinson S, Cordfunke EHP, Konings RJM (1992) Thermochemical data acquisition part 2: joint final report. The Commission of the European Communities, Brussels
13. Mallika C, Sreedharan OM (1990) Standard Gibbs energy of formation of Mo_3Te_4 by EMF measurements. J Nucl Mater 170:246–252
14. Rustamov PG, Abilov CI (1987) Equilibrium diagram of the PbTe–Fe system. Russ J Inorg Chem 32:1016–1018
15. Abilov CI (1989) Projection of the liquidus surface of the Pb–Ni–Te system. Russ J Inorg Chem 34:563–566
16. Wolski K, Laporte V (2008) Grain boundary diffusion and wetting in the analysis of intergranular penetration. Mater Sci Eng A 495:138–146
17. Asl KM, Luo J (2012) Impurity effects on the intergranular liquid bismuth penetration in polycrystalline nickel. Acta Mater 60:149–165
18. Martinelli L, Vanneroy F, Rosado JCD, Hermite DL, Tabarant M (2010) Nickel solubility limit in liquid lead–bismuth eutectic. J Nucl Mater 400:232–239
19. Gossé Stéphane (2014) Thermodynamic assessment of solubility and activity of iron, chromium, and nickel in lead bismuth eutectic. J Nucl Mater 449:122–131
20. Zhang JS (2009) A review of steel corrosion by liquid lead and lead–bismuth. Corros Sci 51:1207–1227
21. Zhang JS, Li N (2008) Review of the studies on fundamental issues in LBE corrosion. J Nucl Mater 373:351–377
22. LaLonde AD, Pei YZ, Snyder GJ (2011) Reevaluation of $PbTe_{1-x}I_x$ as high performance *n*-type thermoelectric material. Energy Environ Sci 4:2090–2096
23. Yang J, Caillat T (2006) Thermoelectric materials for space and automotive power generation. MRS Bull 31:224–229